Inorg. Chem. **2002**, *41*, 981–988

Synthesis and Characterization of a Novel Cyclic Aluminophosphinate: Structure and Solid-State NMR Study

Thierry Azaïs,[†] Laure Bonhomme-Coury,[‡] Jacqueline Vaissermann,[§] Philippe Bertani,[||] Jérôme Hirschinger,[||] Jocelyne Maquet,[†] and Christian Bonhomme*[,†]

Laboratoire de Chimie de la Matière Condensée, Université Pierre et Marie Curie, 4 place Jussieu, 75252 Paris Cedex 05, France, Laboratoire Céramiques et Matériaux Minéraux, ESPCI, 10 rue Vauquelin, 75231 Paris Cedex 05, France, Laboratoire de Chimie des Métaux de Transition, UPMC, 4 Place Jussieu, 75252 Paris Cedex 05, France, and Institut de Chimie, UMR 7510 CNRS, Université Louis Pasteur, 67008 Strasbourg, France

Received July 2, 2001

We present the structure and a multinuclear solid-state NMR study of a new cyclic aluminophosphinate. The crystallographic structure of $[Al_2(HC_6H_5PO_2)_2(C_4H_9OH)_8]Cl_4$ (compound **1**) was obtained at low temperature (a = 11.830(7) Å, b = 14.216(6) Å, c = 17.790(6) Å, β = 91.25(4)°, monoclinic, $P21/c$, Z = 2). ^{13}C IRCP (inversion recovery cross polarization) and NQS (non quaternary suppression) NMR experiments allowed the complete assignment of the quaternary carbon atom of the phenyl ring and the precise determination of the isotropic $|^1J_{P-C}|$ coupling constant. ^{31}P CP MAS dynamics was carefully studied by varying the contact time. Dipolar oscillations even at slow MAS were observed. Up to 11 kHz, these oscillations were more pronounced, and the P–H distance was easily extracted. ^{27}Al NMR quadrupolar parameters for **1** were obtained with very good accuracy, and unusual satellite transition splitting was observed. Furthermore, the isotropic lines of the inner and outer transitions were clearly observable, leading to the unambiguous determination of the quadrupolar parameters.

Introduction

Since the first successful synthesis of crystalline microporous aluminophosphate materials in 1982,[1] these compounds were extensively studied, owing to their catalytic and sorptive properties. The synthetic routes used to prepare metallophosphates are related to hydro- or solvothermal conditions in the presence of an organic template, which acts as a structure directing agent. Recently, a second synthesis approach emerged in the literature: the basic idea is to synthesize clusters with definite cores, corresponding to secondary building units (SBU) of target materials. Further chemical reactions, involving the obtained clusters, would lead to the desired microporous material. The porosity would be determined by the geometry of the cluster's core (building block strategy). Several small alumino- and gallophosphonate entities were successfully synthesized and characterized by X-ray diffraction or spectroscopic techniques, such as IR spectroscopy and solution state NMR. Among them, models for single four ring (S4R),[2] double four ring (D4R),[2d−f,3] prismatic shaped clusters,[2a,e−f] and double six ring (D6R)[4] were reported in the literature. Generally, the synthesis involves the use of phosphonic acids $(RPO(OH)_2$, with R =

* Author to whom correspondence should be addressed. E-mail: bonhomme@ccr.jussieu.fr.

[†] Laboratoire de Chimie de la Matière Condensée, Université Pierre et Marie Curie.

[‡] Laboratoire Céramiques et Matériaux Minéraux, ESPCI.

[§] Laboratoire de Chimie des Métaux de Transition, UPMC.

[||] Institut de Chimie, UMR 7510 CNRS, Université Louis Pasteur.

(1) Wilson, S. T.; Lok, B. M.; Messina, C. A.; Cannan, T. R.; Flanigen, E. M. *J. Am. Chem. Soc.* **1982**, *104*, 1146.

(2) (a) Montero, M. L.; Uson, I.; Roesky, H. W. *Angew. Chem., Int. Ed. Engl.* **1994**, *33*, 2103. (b) Keys, A.; Bott, S.; Barron, A. R. *J. Chem. Soc., Chem. Commun.* **1996**, 2339. (c) Mason, M. R.; Matthews, R. M.; Mashuta, M. S.; Richardson, J. F. *Inorg. Chem.* **1996**, *35*, 5756. (d) Mason, M. R.; Mashuta, M. S.; Richardson, J. F. *Angew. Chem., Int. Ed. Engl.* **1997**, *36*, 239. (e) Mason, M. R.; Perkins, A. M.; Matthews, R. M.; Fisher, J. D.; Mashuta, M. S.; Vij, A. *Inorg. Chem.* **1998**, *37*, 3734. (f) Chandrasekhar, V.; Murugavel, R.; Voigt, A.; Roesky, H. W.; Schmidt, H. G.; Noltemeyer, M. *Organometallics* **1996**, *15*, 918. (g) Browning, D. J.; Corker, J. M.; Webster, M. *Acta Crystallogr., Sect. C* **1996**, *52*, 882. (h) Corker, J. M.; Browning, D. J.; Webster, M. *Acta Crystallogr., Sect. C* **1996**, *52*, 583.

(3) (a) Walawalkar, M. G.; Murugavel, R.; Roesky, H. W.; Schmidt, H. G. *Inorg. Chem.* **1997**, *36*, 4202. (b) Montero, M. L.; Voigt, A.; Teichert, M.; Uson, I.; Roesky, H. W. *Angew. Chem., Int. Ed. Engl.* **1995**, *34*, 2504. (c) Walawalkar, M. G.; Murugavel, R.; Roesky, H. W.; Schmidt, H. G. *Organometallics* **1997**, *16*, 516. (d) Diemert, K.; Englert, V.; Kuchen, W.; Sandt, F. *Angew. Chem., Int. Ed. Engl.* **1997**, *36*, 241. (e) Yang, Y.; Schmidt, H. G.; Noltemeyer, M.; Pinkas, J.; Roesky, H. W. *J. Chem. Soc., Dalton Trans.* **1996**, 3609. (f) Wragg, D. S.; Hix, G. B.; Morris, R. E. *J. Am. Chem. Soc.* **1998**, *120*, 6822. (g) Feher, F. J.; Budzichowski, T. A.; Weller, K. J. *J. Am. Chem. Soc.* **1989**, *111*, 7288.

10.1021/ic010700k CCC: $22.00
Published on Web 02/01/2002

C_6H_5, CH_3, $C(CH_3)_3$) leading to clusters with totally or partially condensed phosphonate groups. The use of diphenylphosphinic acid $(C_6H_5)_2PO(OH)$ as a precursor is reported very rarely, leading to the syntheses of cyclic diphenylgallo- and diphenylaluminophosphinates (S4R).[2g−h] Older references dealing with this type of compounds, describing mainly IR results, may also be noted.[5] Aluminophosphate materials (including $AlPO_4$-n, lamellar, and mesoporous Al−O−P derivatives) were intensively studied by multinuclear solid-state NMR;[6] to our knowledge, SBU analogues have never been investigated by these techniques. However, they can be considered as models for spectroscopic solid-state NMR investigations, as small well-defined molecules are involved. Studying such kinds of clusters by solid-state NMR is promising because of the relationship between the NMR results and the local structure around the studied nuclei. These results are, thus, a perfect starting point for the study of syntheses using the so-called "building block strategy".

We present the study of [bis{μ-phenylphosphinato(−)-*o*,*o*′}bis(tetrabutanolaluminum)]4+ chloride: $[Al_2(HC_6H_5PO_2)_2(C_4H_9OH)_8]Cl_4$ (compound **1**). To the best of our knowledge, it is the first aluminophosphinate cluster, where phosphorus is bonded to a hydrogen atom. The core of the cluster is a cyclic $[Al_2P_2O_4]$ unit, mimicking an S4R unit of microporous derivatives.

After a description of the crystallographic structure, ^{13}C CP MAS data and ^{31}P CP MAS dynamics are presented. Dipolar oscillations were observed, leading to the straightforward determination of P−H distances. This new approach should help for identifying the exact location of protons in inorganic clusters, as well as in inorganic materials. ^{27}Al solid-state NMR data are presented and discussed. Quadrupolar parameters and isotropic chemical shift were obtained by two different strategies: high-speed MAS and full satellite transitions analysis.

Experimental Section

Reagents and Atmosphere. $AlCl_3$ (Prolabo Rectapur), $H(C_6H_5)PO(OH)$ (Aldrich), and *n*-butanol (Prolabo Normapur) were used without further purification. The obtained crystals, corresponding to compound **1**, were highly sensitive to air moisture, leading to complex amorphous derivatives. Therefore, all manipulations concerning these crystals were done in a dried glovebox under argon atmosphere.

Synthesis of $[Al_2(HC_6H_5PO_2)_2(C_4H_9OH)_8]Cl_4$ (1). A 2.00 g (15 mmol) portion of anhydrous $AlCl_3$ was slowly added to 15 mL of cooled (down to 0 °C) *n*-butanol (exothermic reaction). Then, 2.13 g (15 mmol) of $HC_6H_5PO(OH)$ was added to the solution. The vessel was open to air while adding each reagent and then was closed. No special care was taken to control the atmosphere during the reaction process. At 5 °C, colorless crystals of $[Al_2(HC_6H_5PO_2)_2(C_4H_9OH)_8]Cl_4$ (**1**) were obtained after 24 h (5.6 g; 70%). Analyses: C, 47.88; H, 8.66; Al, 5.00; P, 5.90; Cl, 13.09. Calcd. for $C_{44}H_{92}Al_2Cl_4O_{12}P_2$: C, 49.35; H, 8.66; Al, 5.04; P, 5.78; Cl, 13.24. Despite all care taken during the chemical analyses under argon atmosphere, these analyses are not reliable because of the extreme sensitivity of compound **1** toward water traces, which leads to its partial decomposition. Several attempts were made. ^{31}P NMR (121.44 MHz) (field 62.5 kHz, MAS 5 kHz): T_1 54 ± 3 s; $T_{1\rho}(^1H)$ 45 ± 4 ms; $T_{1\rho}(^{31}P)$ 251 ± 40 ms. Thermal analyses: 25−1200 °C, TGA, 77.1 wt % loss (calcd 77.2%); 25−220 °C, TGA, 39.4 wt % loss, DTA, endothermic, *n*-butanol loss; 650−800 °C, TGA, 7.1 wt % loss, DTA, exothermic, phenyl decomposition/combustion; 1220 °C, weak exothermic, crystallization into tridymite ($AlPO_4$) (powder XRD).

Table 1. Crystallographic Data for $[Al_2(HC_6H_5PO_2)_2(C_4H_9OH)_8]Cl_4$, **1**

chemical formula	$C_{44}H_{92}Al_2P_2O_{12}Cl_4$
fw/g mol^{-1}	1070.9
space group	*P*21/*c* (No. 14)
a/Å	11.830(7)
b/Å	14.216(6)
c/Å	17.790(6)
β/deg	91.25(4)
V/Å^3	2991(2)
Z	2
T/°C	−70
λ/Å	0.71069
D_{calcd}/g cm^{-3}	1.18
μ/cm^{-1}	3.27
R^a	0.0926
$R_w{}^b$	0.1146

^{a} $R = \sum||F_o| - |F_c||/\sum|F_o|$. ^{b} $w = w'[1 - ((||F_o| - |F_c||)/6\sigma(F_o))^2]^2$ with $w' = 1/\sum_r A_r T_r(X)$ with 3 coefficients 12.9, 5.09, and 9.72 for a Chebyshev series, for which X is F_c/F_c(max).

Crystallographic Analysis. The selected crystal was rapidly brought out of the corresponding solution and rapidly embedded in Araldite glue under air atmosphere. Data were collected at 203 K under nitrogen atmosphere to avoid decomposition. Accurate cell dimensions (Table 1) and orientation matrices were obtained by least-squares refinement of 25 accurately centered reflections, on an Enraf-Nonius MACH-3 automatic diffractometer equipped with graphite-monochromated Mo Kα radiation. Rather weak decays (≈10%) were observed in the intensities of two checked reflections during data collection; data were accordingly scaled. Computations were performed by using the PC version of CRYSTALS.[7] The data were corrected for Lorentz and polarization effects. No correction absorption was applied. Scattering factors and corrections for anomalous absorption were taken from ref 8. Structure was solved by direct methods (SHELXS[9]) and refined by full-matrix least squares, with anisotropic thermal parameters for all non-hydrogen atoms. Hydrogen atoms were introduced in calculated positions as fixed contributors in the last refinement. The use of 2635 reflections (with $(F_o)^2 > 3\sigma(F_o)^2$ as criterion) to refine 290 parameters led to *R* factors listed in Table 1. Residual electronic density was −0.36 and +0.62 e Å^{-3}. Tables of fractional coordinates, distances, and angles are available as Supporting Information.

(4) Yang, Y.; Walawalkar, M. G.; Pinkas, J.; Roesky, H. W.; Schmidt, H. G. *Angew. Chem., Int. Ed.* **1998**, *37*, 96.

(5) (a) Sangokoya, S. A.; Pennington, W. T.; Robinson, G. H. *J. Organomet. Chem.* **1990**, *385*, 23. (b) Coates, G. E.; Mukherjee, R. N. *J. Chem. Soc.* **1964**, 1295. (c) Weidlein, J.; Schaible, B. *Z. Anorg. Allg. Chem.* **1971**, *386*, 176. (d) Opalinski, H.; Schaible, B.; Weidlein, J. *J. Organomet. Chem.* **1972**, *43*, 107. (e) Schaible, B.; Weidlein, J. *J. Organomet. Chem.* **1972**, *35*, C7. (f) Schaible, B.; Haubold, W.; Weidlein, J. *Z. Anorg. Allg. Chem.* **1974**, *403*, 289. (g) Schaible, B.; Weidlein, J. *Z. Anorg. Allg. Chem.* **1974**, *403*, 301.

(6) (a) Gao, Q.; Xu, R.; Chen, J.; Li, S.; Qiu, S.; Yue, Y. *J. Chem. Soc., Dalton Trans.* **1996**, 3303. (b) Holland, B. T.; Isbester, P. K.; Blanford, C. F.; Munson, E. J.; Stein, A. *J. Am. Chem. Soc.* **1997**, *119*, 6796.

(7) Watkin, D. J.; Prout, C. K.; Carruthers, J. R.; Betteridge, P. W. In *Crystal Issue 10*; Chemical Crystallography Laboratory, University of Oxford: Oxford, U.K., 1996.

(8) Cromer, D. T. *International Tables for X-ray Crystallography*; Kynoch Press: Birmingham, 1974; Vol. IV.

(9) Sheldrick, G. M. *SHELXS86*, Program for the Solution of Crystal Structures; University of Göttingen: Germany, 1986.

Analyses and Spectroscopy. Elemental microanalyses were performed by the Centre d'Analyses CNRS de Vernaison, France. Simultaneous differential thermal and thermogravimetric analyses were performed on a TA Instrument SDT 2960 (air flow, 5 °C/min, 25−1250 °C). Solid-state NMR spectra were recorded on Bruker ASX 200 (4.70 T; Ξ^{31}P, 80.98 MHz), MSL 300 (7.05 T; Ξ^{13}C, 75.43 MHz; Ξ^{27}Al, 78.17 MHz; Ξ^{31}P, 121.44 MHz) and MSL 400 (9.40 T; Ξ^{13}C, 100.57 MHz) spectrometers. Zirconia rotors were used (4 mm). Solid samples were spun at 3−15 kHz. Fluctuations in MAS rotation speed were smaller than ±5 Hz over several hours (±20 Hz for the 4.70 T spectrometer). The magic angle was carefully set by using the ^{79}Br resonance of KBr. Chemical shifts were referenced to TMS via solid adamantane for ^{13}C, 85% H_3PO_4 for ^{31}P, and an acidic aqueous solution of $Al(NO_3)_3$ (1 M) for ^{27}Al. For ^{27}Al NMR spectra, small pulse flip angles (i.e., $\leq\pi/12$)[10] were applied, thus enabling a linear regime of excitation for the spin system. Shift in time of the FID and subsequent baseline correction were applied according to the literature.[11] $T_1(^{31}P)$ were measured by a saturation−recovery experiment (under MAS at 5 kHz). The matching of the Hartmann−Hahn (H−H) condition under moderate MAS (≤5 kHz) was set on adamantane (^{13}C) and compound **1** (^{31}P) (^{1}H 90° pulse duration: 4 μs). Typical relaxation delay was 10 s. For variable rotation speed experiments, the H−H profiles were systematically recorded. Moreover, for a given rotation speed, the H−H condition was periodically checked, especially on the MSL 300 spectrometer. The H−H matching condition was also checked by using the IRCP (inversion recovery cross polarization) sequence: one sets the values of t_{CP} and t_i to give a null signal from the ^{31}P resonance of compound **1**; any change in $B_1(^{31}P)$ (or $B_1(^1H)$) will result in either a negative peak (improved match) or a positive peak (poorer match). This method is sensitive and proves that a slight mismatch of the H−H condition leads to erroneous line intensities using the IRCP sequence. The $T_{1\rho}(^{31}P)$ relaxation time of **1** (at a ^{31}P spin-lock field of 62.5 kHz; MAS at 5 kHz; 7.04 T) and the $T_{1\rho}(^1H)$ relaxation time were measured indirectly by a modified version of the CP experiment.[12] The ^{31}P CP MAS NMR spectra were recorded with 40 different contact times, t_{CP} (35 experiments for ^{13}C IRCP MAS). The NMR experiments under fast MAS conditions (up to 11 kHz) were performed on a Bruker ASX-200. The $n = \pm1$ H−H condition ($\Delta = \omega_1(^1H) - \omega_1(^{31}P) = \pm n\omega_{rot}$) was carefully matched by calibrating the ^{1}H and ^{31}P RF fields directly with compound **1**, using a two-dimensional nutation experiment.[13] The low-power amplifier unit was employed in order to minimize instabilities of RF fields and to have software control on the RF power. Increments of contact time (256) were recorded in the range 0−2.5 ms. Scans (32) were added for each experiment.

Shielding tensor components, as well as second-order quadrupolar line shapes, were obtained by using the WINFIT program developed by Massiot (DM99NT, version available on the web).[14]

Results and Discussion

Structure. Crystallographic data concerning compound **1** are given in Table 1. The core of the complex is a cyclic $[Al_2P_2O_4]$ unit, mimicking an S4R unit of aluminophosphate derivatives (Figure 1). Al and P atoms are located alternatively at the vertices of the cycle, and bridging oxygen atoms link them along edges of the cycle (O1 and O2). Average bond lengths involving the bridging oxygen atoms are Al−O 1.81 Å and P−O 1.50 Å (Table 2). These distances are comparable with bond distances observed in aluminophosphate and -phosphonate clusters. For example, in aluminophosphonate entities such as $[(Me)AlO_3P(t\text{-}Bu)]_6$,[4] $[(i\text{-}Bu)AlO_3P(t\text{-}Bu)]_4$,[3e] and $[(Me)_2AlO_2P(Ot\text{-}Bu)_2]_2$,[15] where *i*-Bu = $CH_2CH_2(CH_3)_2$ and *t*-Bu = $C(CH_3)_3$, the average P−O bond lengths are 1.51, 1.52, and 1.45 Å, respectively; the average Al−O bond lengths are 1.75, 1.76, and 1.78 Å, respectively (single crystal XRD data). In the case of aluminophenylphosphonate derivatives, single crystals are very difficult to obtain, so that the crystallographic structures are usually refined from powder XRD data. For example, the P−O average bond length is 1.53 Å, and Al−O bond

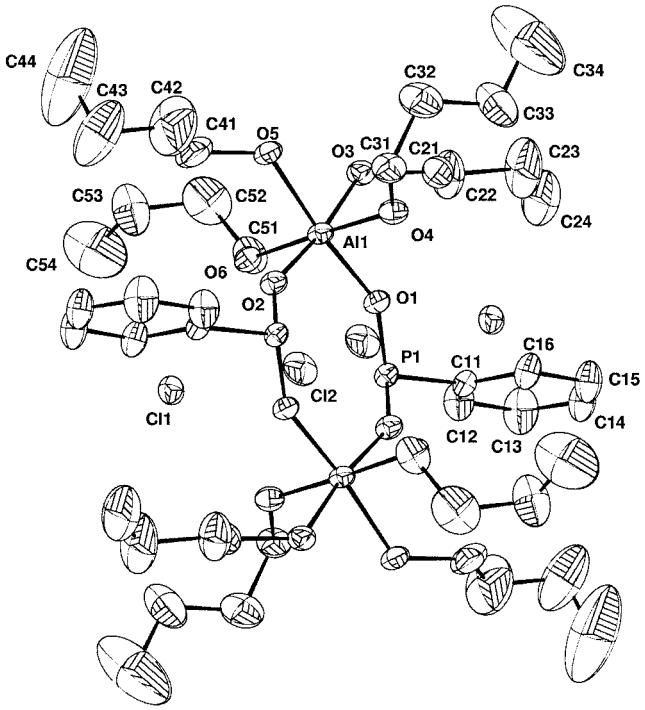

Figure 1. CAMERON drawing of compound **1** (thermal ellipsoids, 20%). The Cl atoms are explicitly shown.

Table 2. Selected Bond Distances (Å) and Angles (deg) for $[Al_2(HC_6H_5PO_2)_2(C_4H_9OH)_8]Cl_4$ **1**

Distances	
Al1−O1	1.812(5)
Al1−O2	1.818(5)
Al1−O3	1.920(5)
Al1−O4	1.913(6)
Al1−O5	1.926(5)
Al1−O6	1.932(6)
P1−O1	1.502(5)
P1−O2	1.503(5)
P1−C11	1.772(7)
Angles	
O1−Al1−O2	98.0(2)
O1−P1−O2	114.1(3)

(10) (a) Man, P. P. *Mol. Phys.* **1993**, *78*, 307. (b) Man, P. P.; Duprey, E.; Fraissard, J.; Tougne, P.; d'Espinose, J.-B. *Solid State Nucl. Magn. Reson.* **1995**, *5*, 181.
(11) Massiot, D.; Müller, D.; Hübert, T.; Schneider, M.; Kentgens, A. P. M.; Coté, B.; Coutures, J.-P.; Gessner, W. *Solid State Nucl. Magn. Reson.* **1995**, *5*, 175.
(12) Jelinski, L. W.; Melchior, M. T. *NMR Spectroscopy Techniques*; Marcel Dekker: New York, 1987; pp 253−329.
(13) Bax, A. *Two-Dimensional NMR in Liquids*; Delft University Press: Delft, 1984.
(14) Massiot, D.; Thiele, H.; Germanus, A. *Bruker Rep.* **1994**, *140*, 43.
(15) Lugmair, C. G.; Tilley, T. D.; Rheingold, A. L. *Chem. Mater.* **1999**, *11*, 1615.

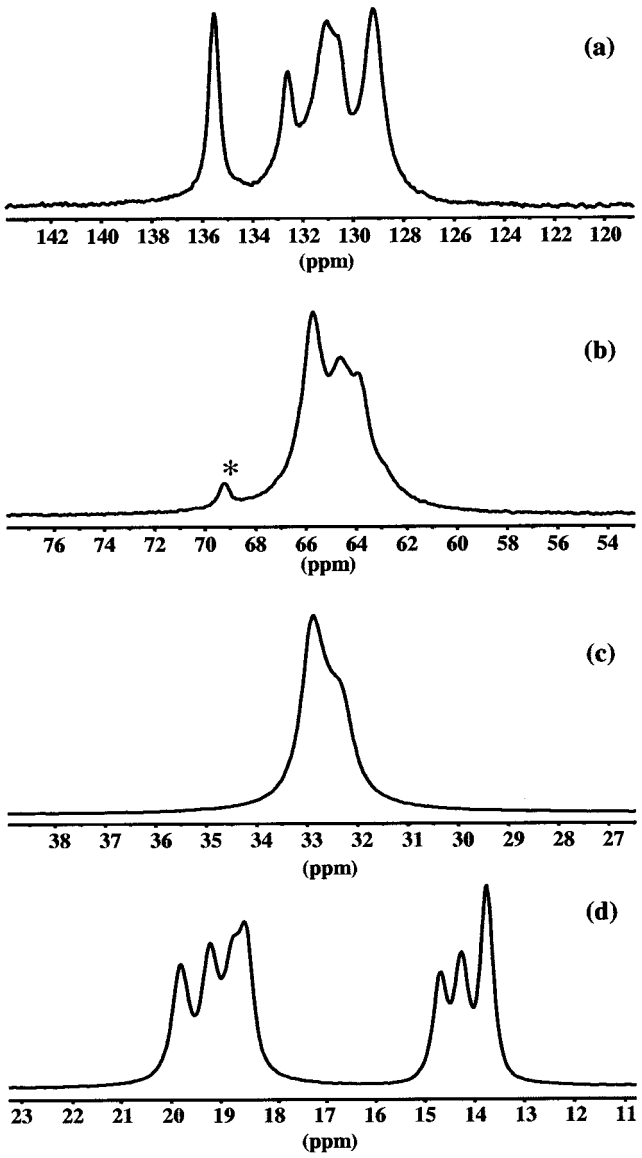

Figure 2. ^{13}C CP MAS experiments for compound **1**: phenyl (a), CH_3-$CH_2CH_2CH_2OH$ (b), $CH_3CH_2CH_2CH_2OH$ (c), $CH_3CH_2CH_2CH_2OH$ (d) on the left, $CH_3CH_2CH_2CH_2OH$ (d) on the right. $\nu_{rot} = 5000$ Hz; $\Xi(^{13}C) = 75.43$ MHz; $N_s = 4000$; $t_{CP} = 3$ ms; recycle delay = 10 s. ^1H high-power decoupling. Asterisk indicates spinning sideband.

lengths vary from 1.79 to 1.95 Å in the lamellar compound α-$Al(HO_3PC_6H_5)(O_3PC_6H_5)\cdot H_2O$.[16]

In compound **1**, a phenyl group and a hydrogen atom complete the tetrahedral coordination of the P atom. The hydrogen position could not be determined by XRD, but the P−H distance could be accurately evaluated by ^{31}P CP MAS experiments (see the NMR section). The phosphinate group ($HC_6H_5PO_2$) is preserved during all the chemical processes. The Al atoms are 6-fold coordinated. Four *n*-butanol ligands are bonded to Al1, and the Al−O average bond length is 1.92 Å. This average length is much longer than the Al−O average bond length observed in aluminum alkoxides (1.80 Å in $[AlO(i\text{-}Bu)]_2[Al(O(i\text{-}Bu))_2]_2[\mu_2\text{-}O(i\text{-}Bu)]_5(\mu_4\text{-}O)H$.[17] The presence of these alcohol molecules prevents the linking

Table 3. ^{13}C, ^{31}P, and ^{27}Al NMR Data for $[Al_2(HC_6H_5PO_2)_2(C_4H_9OH)_8]Cl_4$, **1**, Including Isotropic Chemical Shift (δ_{iso}, ppm), Linewidth (LW, Hz), Quadrupolar Coupling Constant (C_Q, MHz), Asymmetry Parameter (η_Q), Shielding Tensor Components (δ_{ii}, ppm), and Asymmetry Parameter (η_{CSA})[a]

^{13}C	δ_{iso} $CH_3CH_2CH_2CH_2OH$ (LW)	14.74 (24.7); 14.31 (30.5); 13.81 (24.7)
	δ_{iso} $CH_3CH_2CH_2CH_2OH$ (LW)	19.89 (34.2); 19.29 (32.2); 18.83 (32.2); 18.57 (24.3)
	δ_{iso} $CH_3CH_2CH_2CH_2OH$ (LW)	32.96 (46.1); 32.47 (38.3)
	δ_{iso} $CH_3CH_2CH_2CH_2OH$ (LW)	65.76 (70.1); 64.62 (66.0); 63.84 (60.6)
	δ_{iso} C phenyl (LW)	135.51 (50.6); 132.58[f] (57.1); 131.06 (70.1); 130.45[f] (35.0); 129.16 (71.3)
^{31}P	δ_{iso} (LW)	15.3 (115)
	δ_{11}; δ_{22}; δ_{33}[b]	6.7; −10.6; 49.9
	η_{CSA}[b]	0.5
^{27}Al	δ_{iso}	−2.51[c]; −2.49[d]
	C_Q[e]	3.00[c]; 3.03[d]
	η_Q	0.25

[a] δ in ppm; $\delta_{iso} = (1/3)(\delta_{11} + \delta_{22} + \delta_{33})$ with $|\delta_{33} - \delta_{iso}| \geq |\delta_{11} - \delta_{iso}| \geq |\delta_{22} - \delta_{iso}|$; $\eta_{CSA} = (\delta_{22} - \delta_{11})/(\delta_{33} - \delta_{iso})$; $\Delta\delta = \delta_{33} - (\delta_{11} + \delta_{22})/2$. [b] δ_{ii} and η_{CSA} from low speed MAS sideband patterns analysis. [c] From the fitting of the central transition powder pattern under fast MAS (7.04 T). [d] From SORGE diagram (Figure 6 and ref 28). [e] $C_Q = (e^2qQ)/h$; $\delta_{iso}(^{27}Al)^{c,d}$, ±0.1; $\delta_{iso}(^{13}C)$, ±0.02; $\delta_{iso}(^{31}P)$, ±0.1; η_{CSA}, η_Q, ±0.05; $C_Q{}^{c,d}$, ±0.01 MHz. [f] Corresponding to $\delta_{iso} = 131.50$ ppm. $|^1J_{C-P}|_{iso} = (151 \pm 3$ Hz). See text.

of the cycles. Oxygen octahedra surrounding Al atoms are strongly distorted. Furthermore, four chloride anions per cycle are present. They balance the positive charge of the core. The shortest distances between Cl atoms and the oxygens of the alcohol molecules are 2.94 and 2.96 Å, suggesting hydrogen bonding. The lability of the *n*-butanol ligands explains the extreme reactivity of compound **1** toward moisture and air. Nevertheless, this extreme reactivity could be useful for the synthesis of microporous materials by building block strategy.

^{13}C Solid-State NMR Spectroscopy. The ^{13}C CP MAS spectrum of compound **1** (Figure 2) is in agreement with the crystallographic structure. Six aromatic resonances (corresponding to C11 → C16) are expected. Four resonances for each aliphatic carbon molecule are expected as well. The phenyl lines (126 → 137 ppm), the CH_2 lines (17 → 70 ppm), and the CH_3 lines (13 → 16 ppm) are easily assigned (Table 3). Four distinct *n*-butanol molecules are clearly evidenced in Figure 2d: the highest resolution is obtained in the 12 → 21 ppm region, corresponding to the CH_3-CH_2- lines. Special mobility of the chain ends of the butanol molecules is involved, as clearly evidenced by an NQS experiment.[18] The dipolar dephasing is most efficient for the $-CH_2-OH$ sites, in agreement with rigid, strongly coupled CH_2 groups. The dipolar dephasing is strongly reduced for $CH_3-CH_2-CH_2-$ and $CH_3-CH_2-CH_2-$ nuclei. The reduction is also strong for CH_3 groups, because of rapid reorientation.

Several lines overlap in the phenyl region, and an elegant way to assign the quaternary carbon of the phenyl ring is to perform an IRCP experiment,[19] where the ^1H magnetization

(16) Cabeza, A.; Aranda, M. A. G.; Bruque, S.; Poojary, D. M.; Clearfield, A.; Sanz, J. *Inorg. Chem.* **1998**, *37*, 4168.

(17) Sinclair, R. A.; Gleason, W. B.; Newmark, R. A.; Hill, J. R.; Hunt, S.; Lyon, P.; Stevens, J. *Chemical Processing of Advanced Materials*; Wiley-Interscience: New York, 1992; pp 207−214.

(18) Opella, S. J.; Frey, M. H. *J. Am. Chem. Soc.* **1979**, *101*, 5854.

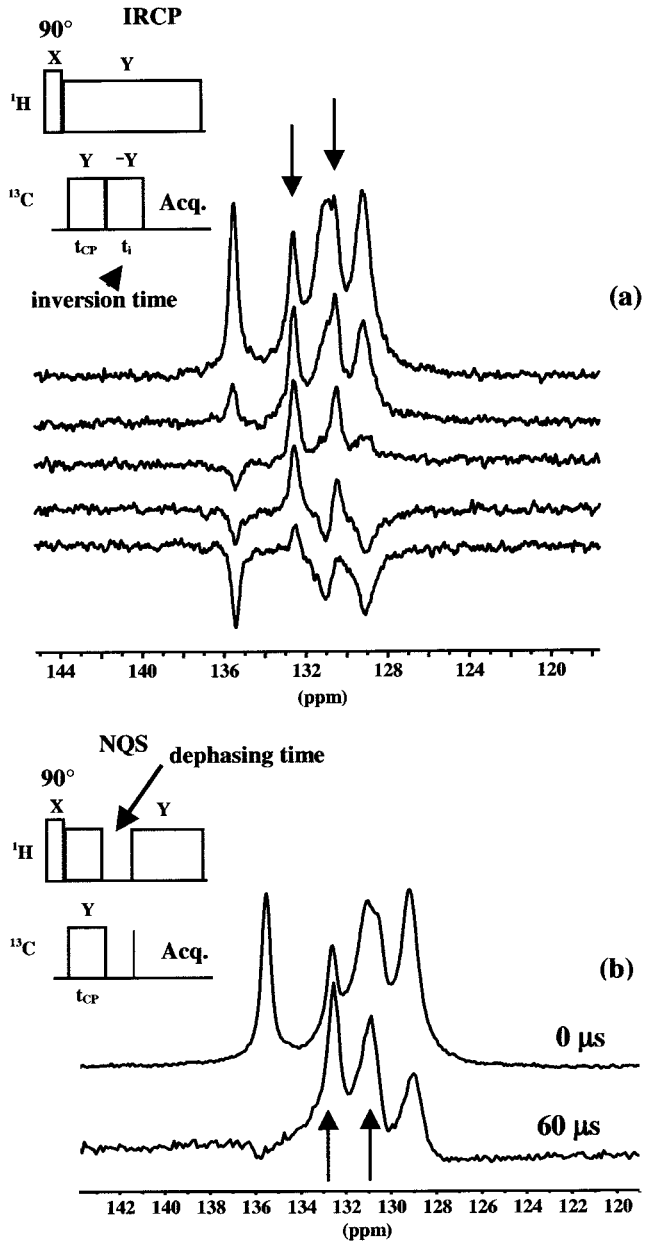

Figure 3. (a) ^{13}C IRCP experiments for phenyl region of compound **1**. Inversion time t_i (from top to bottom): 5 (≈standard CP), 40, 70, 125, 300 μs. Arrows denote the quaternary carbon lines, split by (^{13}C−^{31}P) *J* coupling (see text). ν_{rot} = 5000 Hz; Ξ(^{13}C) = 75.43 MHz; N_s = 240 (for each inversion time value); recycle delay = 15 s. ^{1}H high-power decoupling. (b) NQS experiment for phenyl region of compound **1**, for a dephasing time of 60 μs. ν_{rot} = 4000 Hz; Ξ(^{13}C) = 100.6 MHz; N_s = 2880; recycle delay = 15 s. ^{1}H high-power decoupling.

is first transferred to ^{13}C (CP) in order to polarize all the nuclei. Then, the ^{13}C magnetization evolves with a 180° phase shift (inversion recovery), and the signal is subsequently recorded as a function of the inversion time t_i (Figure 3a). The rate of the inversion of magnetization is directly related to the strength of the dipolar coupling in CH_n groups and is obviously very slow for weakly coupled ^{13}C nuclei (such as quaternary carbon atoms). At $t_i = 70$ μs, two slowly inverting components are clearly observed. They both correspond to the quaternary phenyl carbon atoms, subjected to the (^{13}C−^{31}P) *J*-coupling interaction. Using the IRCP sequence, the $|^1J_{C-P}|_{iso}$ value is therefore easily measured (151 ± 3 Hz) and is in good agreement with constants derived from solution state NMR experiments.[20] This value is fully confirmed by the NQS sequence (Figure 3b).

^{31}P Solid-State NMR. The ^{31}P CP MAS spectrum of compound **1** reveals one unique isotropic line, in full agreement with the crystallographic data. The spectrum at intermediate rotation speed (3000 Hz) allowed the determination of the CSA parameters (Table 3). The cross polarization technique was mainly used to shorten the experimental time (see the T_1(^{31}P) in the Experimental Section). Furthermore, this technique allowed the checking of the spatial proximity between ^{1}H and ^{31}P (direct P−H bond). Using a spinning speed of 5 kHz, the observation of the magnetization curve (versus the contact time, t_{CP}) reveals highly damped oscillations from 125 μs to 1 ms (Figure 4a), which could act as evidence for the spatial proximity between ^{31}P and ^{1}H nuclei. The same experiment performed at 11 kHz shows more pronounced dipolar oscillations (Figure 4b). The spin diffusion process between protons is slowed, and the assumption of an isolated P−H spin pair becomes more realistic. Thus, the P−H distance in the P−H bond is easily extracted after direct Fourier transform of the magnetization curve, leading to a Pake-like doublet in the frequency domain (Figure 4c).[21] The difference (in hertz) between the horns of the Pake-like doublet is directly proportional to the dipolar constant $D_{^1H^{31}P}$ ($\Delta\nu = D_{^1H^{31}P}/\sqrt{2}$), which, in turn, is related to the P−H distance (r_{PH}):

$$D_{^1H^{31}P} = (\mu_0/2\pi)\gamma_{^{31}P}\gamma_{^1H}\hbar/(4\pi r_{PH}^3) \quad (1)$$

A P−H distance of 1.46 ± 0.05 Å is determined (D_{P-H} = 15540 Hz), in agreement with P−H distances already measured in model compounds (such as PH_3).[22] Moreover, this distance is in excellent agreement with the P−H distance previously extracted by this technique in phenylphosphinic acid ($HC_6H_5PO(OH)$) (r_{PH} = 1.46 ± 0.05 Å).[23] The presence of a negative peak in the middle of the doublet (Figure 4c) comes from the $T_{1\rho}$(^{1}H) process, whose effect can be clearly seen on the polarization curve (decreasing of the magnetization at long contact time).[24] This negative peak does not affect the precision of the distance determination, as long as the two horns are clearly visible. Furthermore, sharp peaks at $\pm n\nu_R$ (spinning sidebands), observed on both sides of the doublet, are related to the FT of quasiequilibrium state

(19) (a) Melchior, M. T. *Proceedings of the 22nd Experimental NMR Conference*; Asilomar, 1981; poster B29. (b) Wu, X.; Zhang, S.; Wu, X. *Phys. Rev. B* **1988**, *37*, 9827. (c) Wu, X.; Zilm, K. W. *J. Magn. Reson., Ser. A* **1993**, *102*, 205. (d) Palmas, P.; Tekely, P.; Canet, D. *J. Magn. Reson., Ser. A* **1993**, *104*, 26. (e) Hirschinger, J.; Hervé, M. *Solid State Nucl. Magn. Reson.* **1994**, *3*, 121. (f) Sangill, R.; Rastrup-Andersen, N.; Bildsoe, H.; Jakobsen, H. J.; Nielsen, N. C. *J. Magn. Reson., Ser. A* **1994**, *107*, 67.

(20) Kalinowski, H. O.; Berger, S.; Braun, S. *Carbon-13 NMR Spectroscopy*; John Wiley & Sons: New York, 1988.

(21) Bertani, P.; Raya, J.; Reinheimer, P.; Gougeon, R.; Delmotte, L.; Hirschinger, J. *Solid State Nucl. Magn. Reson.* **1999**, *13*, 219.

(22) *International Tables for X-ray Crystallography*; Kynoch Press: Birmingham, 1968; Vol. III, pp 265.

(23) Azaïs, T.; Bonhomme, C.; Bonhomme-Coury, L.; Vaissermann, J.; Millot, Y.; Man, P. P.; Bertani, P.; Hirschinger, J.; Livage, J. *J. Chem. Soc., Dalton Trans.*, in press.

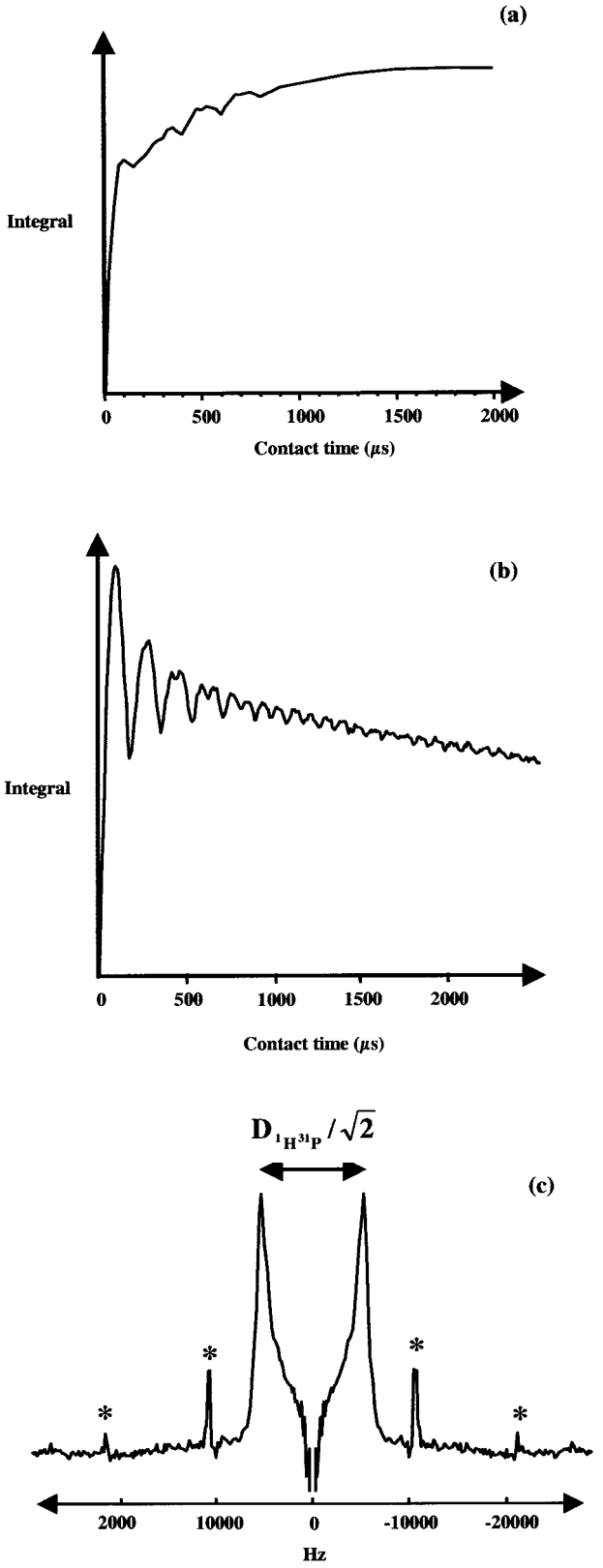

Figure 4. (a) Variable contact time experiments (^{31}P CP MAS) (compound **1**). Total integration of signal versus contact time, t_{CP}. ν_{rot} = 5000 Hz; $\Xi(^{31}P)$ = 121.44 MHz; N_s = 80; recycle delay = 10 s. ^{1}H high-power decoupling. (b) Variable contact time experiments (^{31}P CP MAS) at ν_{rot} = 11000 Hz; $\Xi(^{31}P)$ = 80.98 MHz; N_s = 80; recycle delay = 15 s. ^{1}H high-power decoupling. $n = +1$ H−H condition ($\Delta = \omega_1(^1H) - \omega_1(^{31}P) = \pm n\omega_{rot}$) (^{1}H, 47 kHz; ^{31}P, 36 kHz). See the Experimental Section. (c) Fourier transform of (b) (after multiplication by −1 and zerofilling). Asterisks indicate spinning sidebands (see text).

oscillations (visible as soon as the heteronuclear dipolar P−H oscillations are damped).[24] It must be noted that rotary resonance effects have been previously demonstrated (leading to pseudo-Pake patterns), but in the frame of double-quantum 2D experiments.[25]

^{27}Al Solid-State NMR. ^{27}Al ($I = {}^5/_2$) is a quadrupolar nucleus submitted to a second order quadrupolar interaction, which is not completely averaged by MAS. Consequently, the line shapes obtained for ^{27}Al MAS spectrum are usually complex, broad, but characteristic. The ^{27}Al MAS spectrum of compound **1** shows a unique central resonance exhibiting the features of a second-order quadrupolar line shape (Figure 5a), associated with spinning sidebands (over 1 MHz, Figure 5c). By simulation of the central transition (Figure 5b), the quadrupolar parameters (C_Q, η_Q) and the isotropic chemical shift δ_{iso} are easily extracted (Table 3). The value for δ_{iso} (−2.5 ppm) confirms the octahedral coordination mode of the Al, and C_Q (3.00 MHz) and η_Q (0.25) values confirm the distortion of the oxygen octahedra around the aluminum atoms. The careful observation of the sideband manifold reveals the splitting of the two satellite transitions, the inner transitions ($\pm{}^1/_2$; $\pm{}^3/_2$) and the outer transitions ($\pm{}^3/_2$; $\pm{}^5/_2$) (Figure 5d). The outer transitions are broad and consequently difficult to distinguish. The inner transitions are sharp and clearly visible, with a particular line shape due to the second-order quadrupolar interaction.[26] Furthermore, the isotropic chemical shifts of the inner transitions ($\delta^{<3/2>}{}_{iso}$) and outer transitions ($\delta^{<5/2>}{}_{iso}$) are clearly observed at the foot of the central transition ($+{}^1/_2$; $-{}^1/_2$) (Figure 5a,d). This unambiguous observation was rarely mentioned in the frame of ^{27}Al NMR.[27] It is possible to use these data to confirm the isotropic chemical shift of the central transition, and the quadrupolar constant. Indeed, the center of gravity of each transition ($\delta_{CG}{}^{<m>}$ with $m = {}^1/_2, {}^3/_2, {}^5/_2$) is directly related to δ_{iso} and $\nu_{Q(\eta_Q)}$ where

$$\nu_{Q(\eta_Q)} = \nu_Q\sqrt{1 + \frac{\eta_Q{}^2}{3}} \tag{2}$$

$$\nu_Q = \frac{3}{2I(2I-1)}C_Q \tag{3}$$

The equation relating $\delta_{CG}{}^{<m>}$, δ_{iso}, and $\nu_{Q(\eta_Q)}$ is given by

$$\delta_{CG}{}^{<m>} = \delta_{iso} - [\nu_{Q(\eta_Q)}]^2\frac{[I(I+1) - 3 - 9m(m-1)]10^6}{30\nu_0{}^2} \tag{4}$$

The graphic representation of this equation is called a SORGE diagram (for second-order graphic extrapolation)

(24) Sakellariou, D.; Hodgkinson, P.; Hediger, S.; Emsley, L. *Chem. Phys. Lett.* **1999**, *308*, 381.
(25) (a) Oas, T. G.; Griffin, R. G.; Levitt, M. H. *J. Chem. Phys.* **1988**, *89*, 692. (b) Nielsen, N. C.; Bildsoe, H.; Jakobsen, H. J.; Levitt, M. H. *J. Chem. Phys.* **1994**, *101*, 1805.
(26) Samoson, A. *Chem. Phys. Lett.* **1985**, *119*, 29.
(27) Skibsted, J.; Norby, P.; Bildsoe, H.; Jakobsen, H. J. *Solid State Nucl. Magn. Reson.* **1995**, *5*, 239.

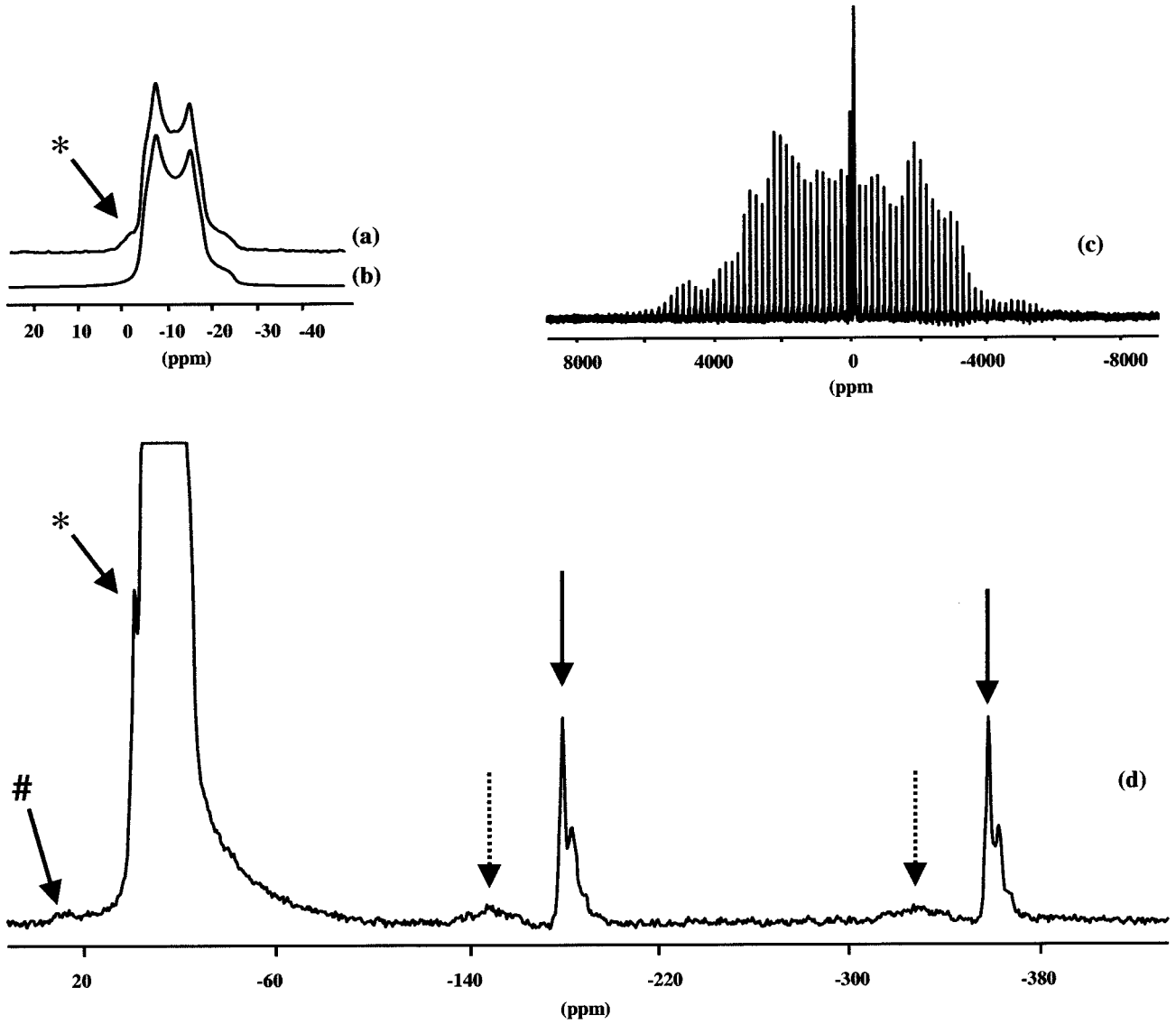

Figure 5. ^{27}Al MAS spectrum of compound **1**. (a) Central transition ($+^1/_2$; $-^1/_2$). (b) Simulation of the second-order broadened transition. (c) Spinning sidebands manifold. (d) Expansion of (c); full arrow denotes ($\pm^1/_2$; $\pm^3/_2$) transitions, broken arrow denotes ($\pm^3/_2$; $\pm^5/_2$) transitions. Asterisk indicates $\delta_{iso}{}^{<3/2>}$; pound sign indicates $\delta_{iso}{}^{<5/2>}$. ν_{rot} = 14000 Hz; $\Xi(^{27}Al)$ = 78.17 MHz; N_S = 7056; recycle delay = 1 s. ^{1}H high-power decoupling.

(Figure 6).[28] The slope of the obtained line gives $(\nu_{Q(\eta_Q)})^2$, and for an "infinite" field, one derives δ_{iso}. The experimental values are $\nu_{Q(\eta_Q)}$ = 466.78 kHz (i.e., C_Q = 3.03 MHz), assuming η_Q = 0.25. These data are in excellent agreement with the previous estimations. This diagram can be used to extract NMR data in the case of compounds where the simulation of the central transition becomes difficult because of line shape distortions.

Conclusion

We have presented a multinuclear solid-state NMR investigation of a new aluminophosphinate compound. The Al−O−P cyclic core mimics a so-called S4R SBU of microporous derivatives. The ^{31}P CP MAS dynamics was carefully studied by variable contact time experiments, realized at different spinning speeds. At 11 kHz, this

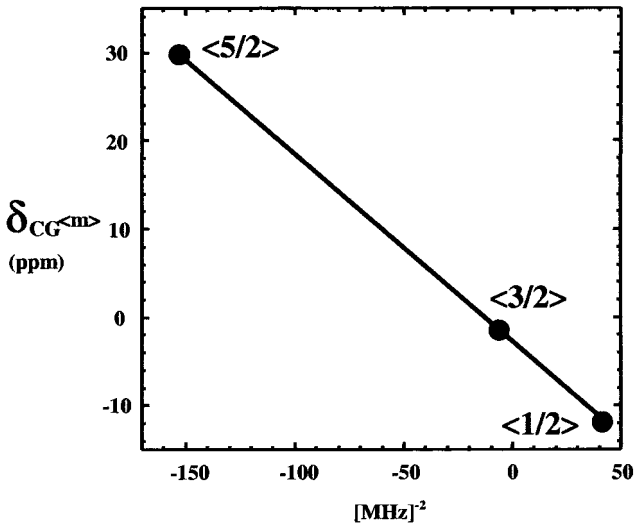

Figure 6. SORGE diagram[28] for compound **1**. $\delta_{CG}{}^{<m>}$ (m = $^1/_2$, $^3/_2$, and $^5/_2$) are plotted versus $X = [I(I+1) - 3 - 9m(m-1)]/30\nu_0{}^2$.

(28) Massiot, D.; Müller, D.; Hübert, T.; Schneider, M.; Kentgens, A. P. M.; Coté, B.; Coutures, J.-P.; Gessner, W. *Solid State Nucl. Magn. Reson.* **1995**, *5*, 175.

technique allows the direct determination of the P−H distance ($d = 1.46 \pm 0.05$ Å in the direct P−H bond). The simplicity of the setup, when compared to other dipolar recoupling techniques such as REDOR[29] or TEDOR,[30] and the development of high-speed MAS probes make this technique very attractive and powerful for the location of hydrogen atoms in aluminophosphate compounds. Very high-speed MAS experiments (up to 33 kHz) and Lee−Goldburg decoupling experiments (leading to isolated spin pairs by quenching of the proton spin diffusion) are now in progress to improve the precision of the measured P−H distances. ^{27}Al experiments converged to the precise determination of NMR parameters (δ_{iso}, C_Q, η_Q). As compound **1** is a well-defined spectroscopic model, such NMR data could be compared to ab initio calculated values soon.

(29) Gullion, T.; Schaefer, J. *J. Magn. Reson.* **1989**, *81*, 196.
(30) Hing, A. W.; Vega, S.; Schaefer, J. *J. Magn. Reson.* **1992**, *96*, 205.

Supporting Information Available: One X-ray crystallographic file, in CIF file. This material is available free of charge via the Internet at http://pubs.acs.org.

IC010700K